

ON FATIGUE CRACK CLOSURE IN STEELS OF DIFFERENT  
MICROSTRUCTURE AND STRENGTH LEVEL

M. Schaper \* and A. Böhm \*\*

Experimental investigations on crack closure in steels with widely different microstructures, strength level (400 to 2500MPa) and threshold behavior are reported. The development of closure during crack growth under K controlled loading procedures as well as after overloading is examined by means of a sophisticated dynamic compliance technique. In general, the results clearly substantiate the expected close correlation between crack closure and the effects of mean load, load sequence and microstructure on fatigue crack growth. On the other hand, some details are not quantitatively accounted for by the simplified  $\Delta K_{eff}$  approach. In view of reliable life prediction, further refinements seem necessary, which should incorporate, e.g., the load sequence dependence as well as the gradual nature of the closure phenomenon.

INTRODUCTION

The crack closure effect describes the phenomenon of mechanical contact in the wake of a fatigue crack, that occurs at above-zero applied loads within a loading cycle. The effect is caused by bridging between the fracture surfaces due to roughness, oxide deposits, residual deformations etc. It is, furthermore, closely related to the internal stress field within the crack tip plastic zone as induced by the applied load range and loading history. The load transfer across the crack faces at above-zero loading lowers the crack tip loading range as compared to the applied one. Thus, the crack closure phenomenon is essentially different from direct internal stress effects in fatigue, which are mean stress effects in nature.

Based on widespread experimental evidence, crack closure is widely accepted to be at least partly responsible for salient features of the fatigue behavior of cracked bodies. The anomalous dependence of the crack propagation threshold on crack size, load ratio, and microstructure as well as the large variety of sequence effects are often ascribed to the crack closure phenomenon. Sometimes even the existence of a threshold is attributed to the closure effect. Nevertheless, conflicting results concerning possible influences of crack length, strength level, loading range, stress state etc. question the validity of the crack closure concept as currently applied. It is argued that the different evaluation procedures are responsible for many of the inconsistencies of published data.

\* Technische Universität Dresden, Institut für Werkstoffwissenschaft, FRG  
\*\* Institut für Festkörper- und Werkstofforschung e.V. (IFW), Dresden, FRG

In the course of about 15 years research activities in the field of fatigue crack growth in ferrous alloys the crack closure effect has been thoroughly analysed in the fatigue laboratory of the IFW by M.Schaper, F.Schlät et al. (e.g. 1-4). In this paper results of an ongoing research on near-threshold phenomena in steels of different types of microstructure and significantly different strength level are presented. Recourse is made to earlier research on overload effects during crack initiation and growth (1).

### EXPERIMENTAL PROCEDURE

Investigated materials. The experiments of the current research program are performed on steels covering a strength range from 400 to 2500 MPa (Table 1). The generalities of the strength level effects are discussed in the following. Specific microstructural aspects will be relied upon in a forthcoming publication.

TABLE 1: Materials used in the current Research Program

Steel	Micro-structure	Chemistry (m-%)							Strength (MPa)		
		C	Mn	Si	Ni	Cr	Nb	Ti	HV5	$R_{el}/R_{p0.2}$	$R_m$
StE355 NbTi	Ferrite- Pearlite	0.07	1.24	0.82	-	-	.022/0.032		153	426	514
X6CrNi Ti 1810	Austenite	0.04	1.11	0.55	9.0	17.0	- 0.32		215	336	623
X210Cr 12	Martensite	2.15	0.3	0.25	-	11.5	- -		806	-	≈2500

The investigations were performed in cantilever bending at a frequency  $f=60$  to 90Hz in laboratory air. Single edge notched specimens with a cross section of  $10 \times 20 \text{mm}^2$  were used. Notches having a depth of about 4.0mm and a root radius of 0.12mm were prepared by spark-machining. For the crack propagation tests a precrack of about 1mm was introduced at  $K_{max} \leq 18 \text{MPa}\sqrt{\text{m}}$ .

Methods of measurement. The crack growth and crack closure experiments were performed by means of DYNACOMP testing machines developed in our laboratory (2,3). With these machines two physical effects are simultaneously used, (a) the resonance effect for low-power excitation of cyclic loading and (b) the dependence of the frequency of resonance vibrations on the masses and (*dynamic*) compliances of a mechanical resonator. A proper design of the set-up not only allows well-defined loading conditions to be realised (including K control) but also enables high resolution compliance analysis. Because the compliance, in turn, is determined by both modulus and geometry of the specimen, crack growth and crack closure can be evaluated without additional instrumentation, i.e. simply by means of vibration period measurements. Furthermore, energy dissipating processes (e.g. specific energy dissipation per crack growth increment) can be derived from measurements of the resonator damping.

The dynamic compliance technique proved to be capable of resolving increments in crack length as small as  $0.5\mu\text{m}$ . Typically, the vibration period,  $T$ , is measured as the mean value over 100 cycles, i.e. every 1 to 2 sec. Depending upon its actual value, the crack growth rate is calculated in intervals of 10sec ( $\approx 750$  cycles), 1min ( $\approx 5000$  cycles), or 10min ( $\approx 50000$  cycles), resp.

The following tests were run: (a) a baseline test series applying different but throughout each test constant  $\Delta K$  levels, (b) threshold measurements under continuous load shedding with  $\Delta K$  control ( $R=\text{const}$ ) or  $K_{\text{max}}=\text{const}$  ( $R$  increasing), resp., with subsequent crack growth rate determination under step-wise load increase, (c) crack initiation experiments after preoverloading notched samples, and (d) overload tests under constant base-line  $\Delta K$  and  $R$ . According to earlier experiments the load reduction rate was kept at  $\delta\Delta K/\delta a \approx 5\text{MPa}\cdot\text{m}^{1/2}/\text{mm}$  or  $C=(1/K)d\Delta K/da = -0,32\text{mm}^{-1}$  in order to avoid load interaction effects (4). The threshold value has been defined for growth rates  $\Delta a/\Delta N \approx 5 \times 10^{-11}\text{m}/\text{cycle}$ .

Crack closure evaluation. In the crack propagation experiments the resonance vibrations are applied both to load the specimen and measure the crack length. An oscilloscopic representation of the electronically integrated acceleration signal versus the instantaneous load (or  $K$  value, resp.) qualitatively exhibits the crack closure intensity within a cycle in this case. For more exact crack closure examination the vibration period serves to characterize compliance changes within preselected cycles. To accomplish this the amplitude of the resonance vibrations is reduced to well below the crack growth threshold. Subsequently, the vibration period is recorded on quasistatically changing the preload between maximum and minimum load of the preceding fatigue cycle. From the corresponding period and preload data crack closure curves are calculated in terms of an effective crack length,  $a_{\text{eff}}$ , versus applied stress intensity,  $K$ .

Sometimes (e.g. McEvily (5)) a significantly higher closure level is reported for the plane stress surface region as compared to the interior even at near-threshold loading, but especially after overloading. Thus, the question arises as to the appropriate measuring technique. Apart from its high sensitivity the above described "far field" method is believed to be superior to near-tip surface measurements, which primarily reveal the plane stress contribution, in that it provides a more realistic estimate of the through-thickness phenomena. Additionally, due to cantilever loading, the compliance measurements are not affected by friction at loading pins or rollers, which interferes in testing CT and SENB specimens.

#### PRINCIPLE FEATURES OF CRACK CLOSURE

As shown in Fig. 1 for low  $R$  and near-threshold loading, the crack may close on unloading down to an effective crack length which - dependent on the loading history - sometimes equals the notch depth. On reloading gradual opening occurs until at an somewhat arbitrarily definable stress intensity,  $K_{\text{op}}$ , the calculated  $a_{\text{eff,max}}$  equals the physical crack length as measured optically on the fracture surfaces. Apart from minor amplitude effects it agrees well with that calculated from the vibration period of the foregoing high amplitude loading. The basic similarity to *differentiated* conventional load-displacement curves,  $F(\delta, \text{ or } s)$ , is obvious from the comparison depicted in Fig. 1, where the displacement is measured by means of a clip gauge mounted at the side surface just behind the crack tip (4).

In spite of the superior sensitivity of the dynamic compliance technique, one of the crucial questions of the crack closure community arises again, i.e. that concerning an unambiguous and mechanically meaningful measure of the crack closure effect. Therefore, we determined two limiting values of  $K_{\text{op}}$ . Consistently with the often applied practice the upper limit is defined at first deviation from the

open crack compliance, but the lower limit through the intersection of the tangents on the curves in the transition to partial closure. This follows our earlier suggestion (e.g. (4)) that a reliable measure of  $K_{op}$  should include some part of the gradual opening into  $\Delta K_{eff}$ . The evaluation procedure proposed by Chen, Weiss and Stickler (6) turned out to be not unambiguously applicable.

#### PECULARITIES OF THE CRACK CLOSURE PHENOMENON

Several interesting physical phenomena were observed to interfere (Fig.2) and should be considered in the interpretation of closure measurements:

- (a) In the upper part of the prior fatigue cycle a slight decrease in the vibration period is often observed when approaching  $K_{max}$ . This indicates a loss of compliance which might be due to an exhaustion of the mobility of the dislocations within the plastic zone. Accordingly, this effect is observed primarily in lower strength coarse grained materials.
- (b) In the lower part of the fatigue cycle, where partial closure occurs, an enhanced sensitivity of the vibration period to small vibration amplitudes is observed. This indicates some form of adhesive fretting between the fracture surfaces. Correspondingly, enhanced damping and specific energy dissipation has been measured during crack propagation at low R when approaching the threshold by load shedding (8).
- (c) When crack closure is measured down to full unloading after fatiguing at high R, the compliance drops immediately below  $K_{min}$  of the preceding cycle, but on reloading the crack opens at much lower stress intensities. This effect is caused by (partial) elimination of asperities in the crack wake and, consequently, occurs primarily on the first unloading, but partly recovers after some crack advance. It indicates a dependency of the closure behavior on the loading conditions and implies that closure under nonstationary loading should be influenced by the minimum load or  $K_{min}$ , resp.
- (d) Apart from an overall but minor amplitude dependence of the vibration period (crack tip plasticity, external damping etc.) an additional effect appears when covering different amounts of closure. If necessary, the latter effect is eliminated by measuring the period over the open part of the cycle (3), whereas the first one can be minimized by proper data evaluation schemes.
- (e) During crack propagation after overloading a transitional hump appears in the crack closure curves due to the occurrence of two closure levels (see below).

#### CRACK CLOSURE UNDER STEADY-STATE CONDITIONS

As a base-line experiment we analysed the crack closure behavior during crack propagation at constant  $\Delta K$  and low load ratio ( $R=0.05$ ). Results for the three types of steels are very similar. Fig.3 represents a typical example for the corresponding crack closure curves. In the initial Paris regime the  $K_{op}$  values were found to be slightly higher than  $K_{min}$  but roughly constant throughout each test. Especially, no indication for a separate influence of the applied stress (bending moment) is evidenced. On the other hand, the values of  $K_{op}/K_{max}$  and U revealed the marked difference in the strength level in that the  $K_{op}$  values were significantly lower in the martensitic steel. Such behavior can be rationalized, if a competition between COD and residual displacements controlled the amount of crack closure with non-equal stress relaxation around both crack faces (e.g. due to secondary cracking) being suggested to intensify the wedge, especially in the plane strain interior.

Fig.4 is a typical representation of  $da/dN(\Delta K)$  curves of the second test series which has been conducted under continuous  $\Delta K$  shedding at  $R=\text{const}$  and subsequent step-wise  $\Delta K$  increase as well as under  $K_{\text{max}}=\text{const}$ . An example of crack closure curves measured during shedding at three different load ratios is depicted in Fig.5 for the ferritic-pearlitic steel. It is seen that the  $K_{\text{op}}$  value remained roughly constant throughout the test, a behavior which is in accord with the master curve of McClung (7) for the threshold region, but contradicts his generalization for the Paris regime. On the other hand,  $K_{\text{op}}$  slightly decreased on  $\Delta K$  shedding at  $R=0.05$  for both the martensitic and austenitic steels, which means that  $K_{\text{op}}$  is in some way related to the applied  $K_{\text{max}}$  or  $K_{\text{min}}$ . This behavior seems plausible for the high strength, but highly brittle martensitic material used in this investigation and is probably caused by the suppression of stage I like growth due to the very fine microstructure as well as by interfering monotonic fracture modes. Additional investigations are now under way in order to clear the factors controlling the threshold behavior of the austenitic specimens.

The threshold results are summarized in Fig.6. At large R an unique threshold value is observed, irrespective of the large differences in microstructure and strength level. On the other hand, there is a clear difference in the load ratio dependence with the two extremes of the ferritic-pearlitic steel showing the strongest ( $\Delta K_{\text{th}}$  seems to be  $K_{\text{max}}$  controlled below  $R=0.6$ ) and the martensitic steel exhibiting an almost negligible influence. In spite of its low strength level, the austenitic steel is characterised by a comparatively weak R effect, which parallels the observation of almost no oxide deposit formation. Although more decisive, these results are in general agreement with the majority of published data as well as earlier findings on a wide range of steels and other iron-base alloys (e.g. 8).

TABLE 2: Nominal and effective Threshold Values for the three Steels with significantly different Microstructures (viz. Table 1). The Boundary Values of  $\Delta K_{\text{th,eff}}$  are derived from different  $K_{\text{op}}$  Definitions

Material	R=0.05		R=0.50		$K_{\text{max}}=\text{const}$ $\Delta K_{\text{th}}=\Delta K_{\text{th,eff}}$ (MPa√m)
	$\Delta K_{\text{th}}$ (MPa√m)	$\Delta K_{\text{th,eff}}$ (MPa√m)	$\Delta K_{\text{th}}$ (MPa√m)	$\Delta K_{\text{th,eff}}$ (MPa√m)	
StE355 NbTi	7.92	5.0...4.0	3.5	3.5...3.3	3.1
	7.88	5.3...4.2			3.0
X6CrNiTi1810	4.42/4.82	2.5...2.4	4.79	4.7...3.5	3.0
	4.90	3.6...3.0			
X210Cr12	3.35/3.5	2.4...1.8	3.46	3.5...3.4	3.2
	3.89	2.6...2.1			

Table 2 exemplifies the general finding that the load ratio influence is not consistently accounted for by the closure effect. Obviously, the conventional closure definition overestimates the influence of closure on the threshold condition at least for the martensitic steel in that its effective threshold at low R becomes smaller than that measured at  $R \geq 0.8$ , where crack closure within the fatigue cycle was found to be completely suppressed. On the contrary, our results for the ferrite-pearlite are roughly consistent with an effective threshold value of about  $3\text{MPa}\sqrt{\text{m}}^{1/2}$ . Furthermore, the observed resistance curve behavior of the threshold value at low R for both the ferritic-pearlitic and the austenitic steels further strengthens the closure argument. In agreement with experiments performed by Pippan et al. (9) we found a

gradual built-up of crack closure under  $R=0.05$  cycling during more than 1mm crack growth after its elimination by intermittent compression cycling (Fig.7). Accordingly, even in long term tests only limited crack advance is achieved on cycling in-between  $\Delta K_{th,eff}$  and  $\Delta K_{th}$ .

Regarding some confusing results and discussions in the literature the following findings of related investigations performed in our laboratory should be mentioned:

- (i) Effects which can be rationalized in terms of crack closure include the extraordinary high threshold values of precipitation hardenable FeCu alloys found after underaging ( $K_{max,th} \approx 18\text{MPa}\sqrt{\text{m}}$ , (8)), the occurrence of a minimum in the temperature dependence of the threshold at about 200°C for ferritic-pearlitic steels (10), enhanced threshold values in oxidizing environments (8) etc.
- (ii) A rough fracture surface topography is not per se connected with intensified crack closure and an enhanced threshold value. In an earlier study we observed very large fracture tortuosity in FeNi alloys after severe artificial grain boundary embrittlement without effects on the threshold value. On the other hand, the superior threshold values of underaged coarse grained FeCu alloys mentioned above were caused by a distinctly stepped fracture path due to transgranular strain localization (1,8). The difference between these two findings originates from the different micromechanisms of crack growth and the resulting contributions of mode II displacements.

### CRACK CLOSURE AFTER OVERLOADING

Crack closure after preloading of notched specimens. The role of crack closure during initial crack growth in a compressive residual stress field has been analysed on sharply notched specimens ( $\rho=0.12\text{mm}$ ) of a HSLA steel after preloading up to a stress intensity  $K_{\sqrt{}}=58\text{MPa}\sqrt{\text{m}}$  (1). When increasing the preload an enhanced fatigue limit is measured. Simultaneously, an enlarged region of initially reduced growth rate is observed together with an enhanced closure level (up to three times the steady-state value), which diminishes as the crack grows through the preload affected zone. A typical example for the development of crack growth and crack closure just above the fatigue limit ( $R=0$ ) is depicted in Fig.8. In spite of the qualitative correlations, two inconsistencies remain with respect to the  $\Delta K_{eff}$  approach: (a) the affected crack length is larger than the calculated preload plastic zone (b) no unique growth rate curve with the steady state Paris line is achieved on the basis of  $\Delta K_{eff}$  (Fig.9).

Crack closure after single tensile overloads. The overload retardation is revealed by the alteration in the closure behavior (e.g.(1) and (3)). After some crack growth following an overload, two opening events are resolved, similarly as in (5,6). During unloading from  $K_{max}$  closure initially occurs at an enhanced  $K_{op,u}$ , but only to the crack length corresponding to the that at the overload application. Further closure requires additional unloading and occurs below a second  $K_{op,l}$  which is lower than the steady state value before the overload. Once crack growth recovers the steady-state rate the upper opening level approaches that which would have prevailed in the absence of any sequence effect and the lower  $K_{op}$  disappears. The lower opening level is completely suppressed, if an overload near general yielding is applied (Fig.10). This behavior is in accord with the picture of an initial acceleration due to crack tip blunting (11) and reflects the residual displacement left in the wake of the advancing crack independent on whether stress state (13) or closure distance effects (5,7) are considered as responsible for the two opening levels.

Earlier experiments (1) on two steels with largely different strength level have shown that the overload affected crack length is not generally related to the overload plastic zone size but could be much larger as found for a high strength martensitic steel. In both steels a quantitatively similar retardation has been observed, which contradicts the constraint effects sometimes claimed. At least in its later stage, the intensity and extent of the retardation phenomenon is, therefore, explained as being primarily due to crack closure as influenced by residual displacements far behind the crack tip in spite of the fact that its interpretation in the usually applied simplified  $\Delta K_{\text{eff}}$  approach does not work sufficiently. The delay is attributed to the initial relaxation of the compressive residual stresses (14) within the overload-affected zone and the intensification of closure with increasing closure length (a gradual rise of  $K_{\text{Op}}$  is not necessary to be assumed).

### SUMMARY AND CONCLUSIONS

From the results of our investigations the following conclusions can be drawn:

1. Whereas the ferritic-pearlitic steel exhibits a strong influence of the load ratio on the threshold value, this effect is largely reduced in the investigated austenitic and martensitic steels. An unique threshold of about  $3\text{MPa}\sqrt{\text{m}}$  is measured at  $R \geq 0.8$ .
2. Crack closure is not a prerequisite for the existence of a threshold value, i.e. there is a non-zero effective threshold for all the materials investigated.
3. At least for the ferritic-pearlitic steel,  $K_{\text{Op}}$  is roughly independent on the length of macrocracks for  $\Delta K = \text{const}$  cycling in the Paris region. Correspondingly, the ratio  $K_{\text{Op}}/K_{\text{max}}$  is found to decrease with increasing  $K_{\text{max}}$ , i.e.  $U = \Delta K_{\text{eff}}/\Delta K$  increases.
4. The conventionally defined  $K_{\text{Op}}$  is probably influenced by  $K_{\text{min}}$  and, therefore, depends on the R ratio. It is slightly enlarged at higher R, which means that the ratio  $K_{\text{Op}}/K_{\text{max}}$  for a given  $K_{\text{max}}$  is higher at higher R.
5. A dual-type closure behavior develops after preoverloading of notched samples as well as after intermittent overloads. The lower opening point is completely eliminated following overloads near general yield.
6. Despite the overall correlations found, the effects of mean load and load sequence on fatigue crack growth are not quantitatively accounted for solely on the basis of the simplified  $\Delta K_{\text{eff}}$  approach. Inconsistencies remain which confirm the occurrence of cyclic damage below  $K_{\text{Op}}$  as usually defined. There is evidence for intrinsic mechanisms and mean stress effects to play a direct role in determining both crack tip loading state and crack growth resistance.
7. Additional round-robins are highly recommended in order to develop a generally acceptable procedure for crack closure measurements and data evaluation.

### REFERENCES

- (1) F. Schlät and M. Schaper, ICMFMM-7, Miskolc, 1983, Publ. Techn. Univ. Miskolc C 39 1983, Vol. C 39, pp. 173-187 and Vol. C38, pp.157-173
- (2) F. Schlät, M. Schaper, Proc. 9th Congr. Materials Testing, Ed. E.Csoboly, Technoinform, Budapest, 1986, Vol.1, pp. 109-113
- (3) M. Schaper, F. Schlät, Wiss. Berichte ZFW Dresden, 1988, Vol.39, pp.39-56
- (4) M. Schaper, A. Böhm, F. Schlät, A. Tkatch, Proc. 10th Congr. Materials Testing, Ed. E.Csoboly, GTE, Budapest, 1991, Vol.2, pp. 556-571
- (5) McEvily, A.J. and Yang, Z., in FATIGUE 90, Vol.1, pp.23-36
- (6) Chen, D.L., Weiss, B., Stickler, R., Int. J. Fatigue, 1991, Vol.13, pp.327-331
- (7) McClung, R.C., Metall. Trans. A, Vol. 224, 1991, pp.1559-1571



- (8) M. Schaper, F. Schlät, ECF-7, EMAS, Ed. E. Czoboly, Vol.2, pp.1072-1080
- (9) Pippan, R., Plöchl, L., Klanner, F., Materialprüfung 1993, Vol.35, pp.333-338
- (10) Schaper, M., Research Report, ZFW Dresden, 1989
- (11) Vormwald, M. and Seeger, T., Fat.Eng.Mat.Struct. 1991, Vol.14, pp.205-225
- (12) P.C.Paris and L.Hermann, in "Fatigue Thresholds", J.Backlund, A.F.Blom, C.J.Beevers, eds., EMAS, 1982, Vol.1, pp.11-32
- (13) McEvily, A.J. and Yang, Z., Met.Trans.A, 1990, Vol. 21A, pp.2717-2727
- (14) C.M.Ward-Close and R.O.Ritchie, in "Mechanics of Crack Closure", J.C.Newman,Jr. and W.Elber, eds., ASTM STP 982, 1988, pp.93-111

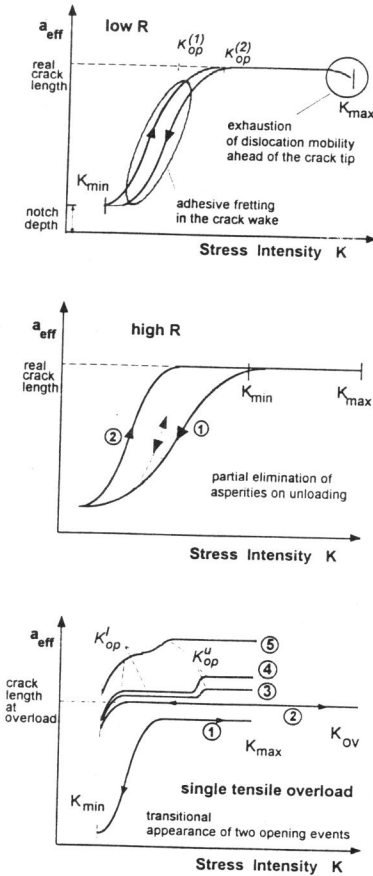


Fig. 2: Peculiarities of the crack closure phenomenon, schematically

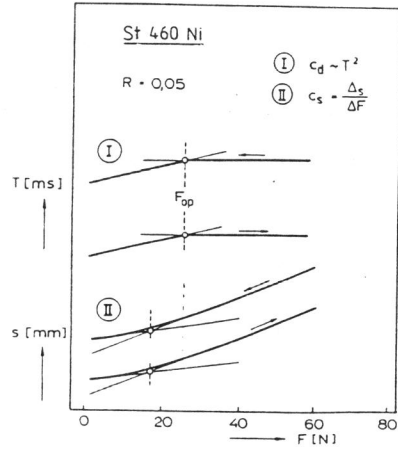


Fig. 1: Closure evaluation by means of dynamic (I) and static (II) compliance measurements

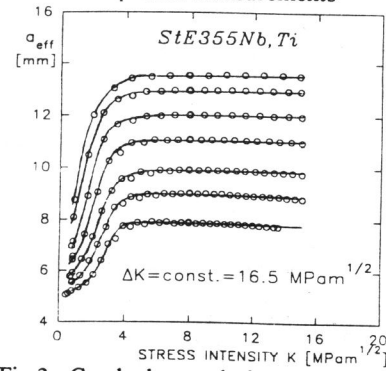


Fig. 3: Crack closure during crack growth at  $\Delta K = \text{const}$ ,  $R = 0.05$ , ferritic-pearlitic steel



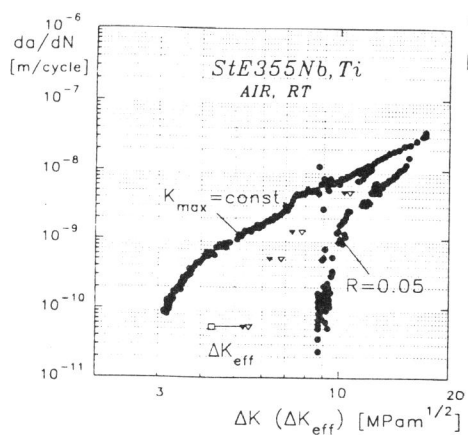


Fig. 4: Crack growth curves for  $R=0.05$  and  $K_{max}=const$ ,  $\Delta K_{eff}$  indicated, ferritic-pearlitic steel

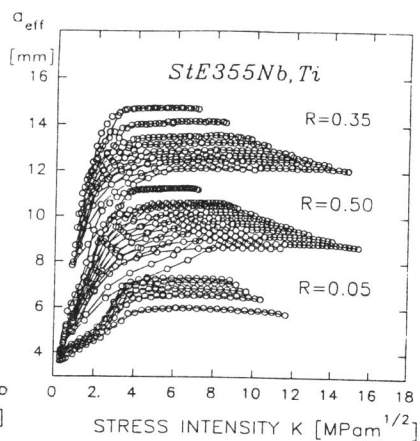


Fig. 5: Crack closure during load shedding at different load ratios, ferritic-pearlitic steel

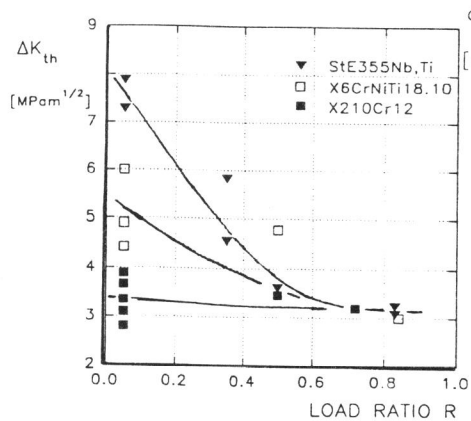


Fig. 6: Load ratio dependence of nominal threshold values for the ferritic, austenitic and martensitic steels, resp.

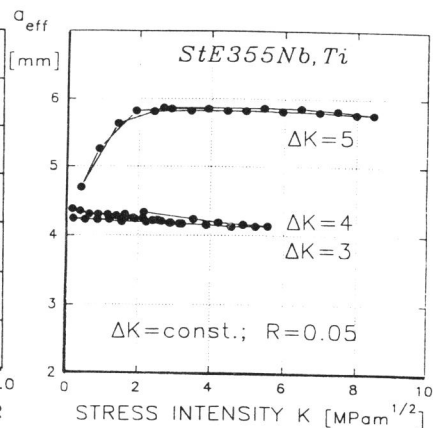


Fig. 7: Crack closure during initial crack growth above  $\Delta K_{th,eff}$  ( $R \approx 0$ ) following compression cycling

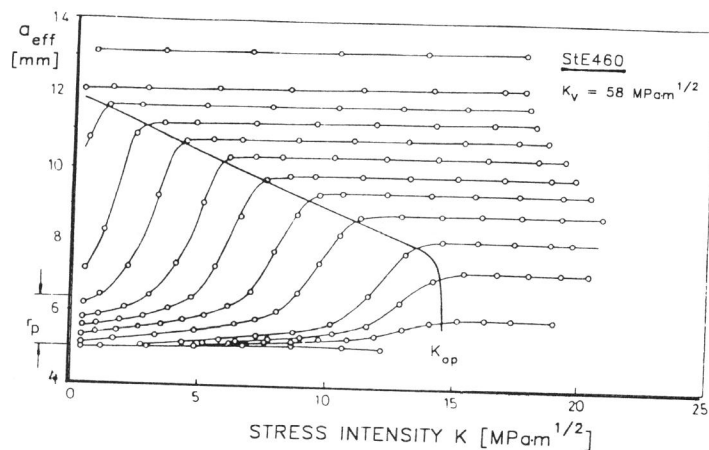


Fig.8: Crack closure for a crack emanating from a sharp notch after application of a preload near net-section yielding,  $r_p$ -preload plastic zone size

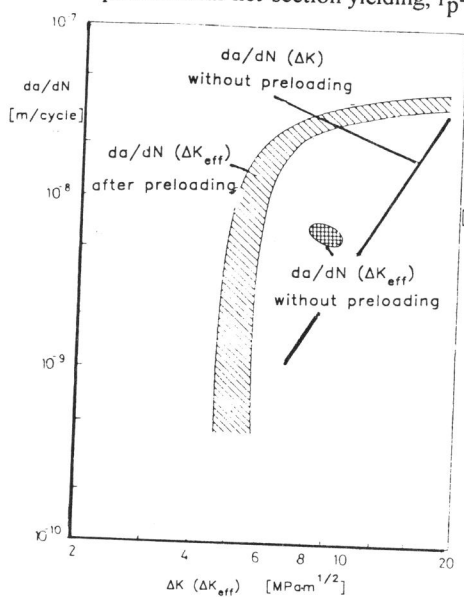


Fig.9: Growth rate after prestressing the notched specimen, compared to steady-state conditions

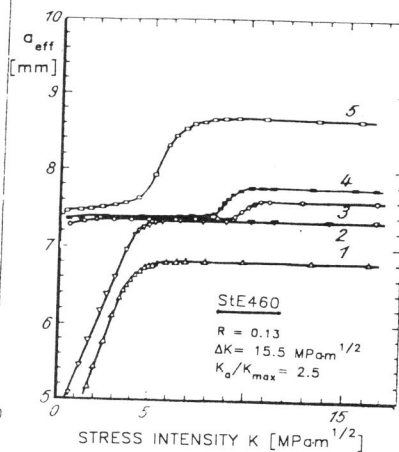


Fig.10: Crack closure following an overload near net-section yielding  $K_{ov}/K_{max}=2.5$ ; C-Mn steel